Genome–Wide Identification, Characterization and Expression Profiling of YUCCA Family Genes Responsive to Exogenous Hormones and Abiotic Stress in Peanut

Chuheng Li , Songyuan Li , Jiabao Wang , Liguo Guo , Guanglei Tang , Yuewei Quan , Charles Y. Chen , Xinlei Yang *

Posted Date: 15 December 2025

doi: 10.20944/preprints202512.1329.v1

Keywords: peanut; YUCCA; bioinformatics; expression analysis

 doi:10.20944/preprints202512.1329.v1

Article

Genome–Wide Identification, Characterization and Expression Profiling of YUCCA Family Genes Responsive to Exogenous Hormones and Abiotic Stress in Peanut

Chuheng Li [1], Songyuan Li [1], Jiabao Wang [1], Liguo Guo [1], Guanglei Tang [2], Yuewei Quan [2], Charles Y. Chen [3] and Xinlei Yang [1,*]

[1] State Key Laboratory of North China for Crop Improvement and Regulation, North China Key Laboratory for Crop Germplasm Resources of Education Ministry, Key Laboratory of Crop Germplasm Resources of Hebei Province, Hebei Agricultural University, Baoding 071001, China

[2] Handan Academy of Agricultural Sciences, Handan, Hebei 056000, China

[3] Department of Crop, Soil and Environmental Sciences, Auburn University, Auburn, AL 36849, USA

* Correspondence: peanut@hebau.edu.cn; Tel.: +86-312-7528136

Abstract

YUCCA (YUC) proteins, serve as crucial rate-limiting enzymes of the tryptophan-dependent auxin biosynthesis pathway, and play essential roles in plant growth, development, and stress adaptation. As of now, a comprehensive examination of the YUC gene family in peanut remains insufficient. In this study, a total of 89 YUC family genes, named *AdYUC1-AdYUC25*, *AiYUC1-AiYUC21* and *AhYUC1-AhYUC43*, were identified within *A. duranensis*, *A. ipaënsis* and *A. hypogaea* genomes and classified into five phylogenetic clades (Clade I - V). The gene structures and protein motifs were conserved among the majority of *AhYUCs*. Collinearity analysis indicated that substantial segmental duplication events contributed to the expansion of the *AhYUCs*, and the majority of duplicated gene pairs underwent strong purifying selection. Promoter prediction analysis detected 3,903 *cis*-acting elements associated with plant growth and hormone, stress and light responsive. *In silico* expression profiling of 43 *AhYUCs* across 22 tissues showed different spatial and temporal expression patterns, with 15 *AhYUCs* has significant expression difference. Meanwhile, base on previous transcriptome data of lateral branches development, *AhYUC9*, *AhYUC18* and *AhYUC29* were identified. Subsequently, the expression patterns of the 8 *AhYUCs* were analyzed using quantitative real-time polymerase chain reaction (qRT - PCR) under treatments of PEG, NaCl, ABA, GA_3, and 6-BA. Notably, *AhYUC18* and *AhYUC29* also exhibited significant trends under different treatments in two genotypes, which speculated to potentially participate in the growth-survival balance in peanuts. This study provides a valuable foundation for the functional characterization of *AhYUC* genes in peanut growth and stress physiology.

Keywords: peanut; YUCCA; bioinformatics; expression analysis

1. Introduction

Auxin, as a vital endogenous hormone in plants, exerts a pivotal function in regulating growth and development processes and responding stress resistance [1]. This function depends on the precise coordination of multiple processes, encompassing auxin biosynthesis, metabolism, transport, and signal transduction [2]. Throughout the plant life-cycle, indole-3-acetic acid (IAA) participates in regulating nearly all plant tissues development processes [3–8]. Moreover, the maintenance of auxin homeostasis is indispensable for plants to cope with abiotic stresses, such as salt stress and drought

 doi:10.20944/preprints202512.1329.v1

stress [9]. The biosynthesis of IAA in plants is primarily achieved through tryptophan (Trp)-dependent and Trp-independent pathways. Among these, the Trp-dependent pathway has been the most extensively investigated [10]. This pathway consists of four main branches, yielding different intermediate products: tryptamine (TAM), indole-3-pyruvate (IPA), indole-3-acetaldoxime (IAOx) and indole-3-acetamide (IAM) [11]. Among them, the IPA pathway is regarded as the principal pathway for plant IAA synthesis. Specifically, Trp is initially catalyzed by Trp aminotransferase (TAA) to generate IPA, and then the YUCCA protein catalyzes the rate-limiting and irreversible step of converting it to IAA [12].

YUC proteins are classified as class B flavin-containing monooxygenases (FMOs). Current plant genome data indicate that only class B FMOs exist in plants [13]. Previous efforts have revealed that YUC proteins possess multiple conserved motifs, including FAD-binding motif, FMO-identifying sequence, NADPH-binding motif, ATG-containing motif 1 and ATG-containing motif 2 [14]. Among these motifs, the FAD-binding motif and NADPH-binding motif form the catalytic core of YUC proteins, and all YUC members contain these two motifs. The FMO-identifying sequence serves as a crucial recognition sequence for plant FMOs, which promotes the binding of NADPH [15]. To date, genome-wide identification of the *YUC* gene family has been accomplished in numerous plants, such as *Arabidopsis* (11), rice (14), maize (14), wheat (25), soybean (22), alfalfa (11), cucumber (7), Isatis indigotica (10), Mikania micrantha (11), cotton (22), and mung bean (11) [16–26]. The biological functions of *YUC* have been elucidated in some species, especially in model plants. Zhao et al. [27] initially discovered that the *Arabidopsis* FMO protein YUC can participate in auxin biosynthesis by catalyzing a key step in the Trp-dependent pathway, thereby revealing the role of FMO-like enzymes in plant auxin synthesis. Cheng et al. [16] indicated that although single *YUC* gene mutants in *Arabidopsis* do no display obvious phenotypic abnormalities, *YUC1* and *YUC4* double mutants exhibit significant phenotypes such as reduced number of floral organs; whereas YUC quadruple mutants completely lose the ability to form floral organs and vascular systems, validating the functional redundancy and specificity of *YUC* family genes at the organ level. Chen et al. [28] demonstrated that *YUC* gene-mediated local auxin synthesis in roots is essential for primary root elongation and gravitation establishment.

In addition, the expression of *YUC* genes is regulated by various internal and external factors, including light signals, hormone signals, and stress, suggesting that they also play significant roles in plant adaptation to environmental alterations [29]. For example, Yang et al. [22] characterized the expression patterns of 10 *CsYUCs* in cucumber under distinct stress treatments, demonstrating that different members participate in different stress responses. They also verified that *CsYUC11* results in pedicel elongation due to excessive auxin accumulation, thereby enhancing drought resistance. Wang et al. [25] systematically identified the *YUC* gene family in five cotton species and silenced *GhYUC22* via virus-induced gene silencing (VIGS). The findings indicated that silencing of this gene decreased reactive oxygen species (ROS) levels and enhanced abscisic acid (ABA) signaling, improving drought resistance. Sun et al. [30] discovered that under high-temperature induction, overexpression of *Arabidopsis YUC8* leads to hypocotyl elongation. Lee et al. [31] found that under drought induction, the *YUC7-1D* mutant exhibits elongated lateral roots to resist drought stress . In the context of heavy metal stress, Liu et al. [32] observed that the expression level of *YUC* genes in the root tip transition zone of *Arabidopsis* increases, and the auxin content in this region increases, inhibiting the growth of *Arabidopsis* lateral roots in response to aluminum ion stress.

Peanut (*Arachis hypogaea* L., 2n = 4x = 40, AABB), or groundnut belongs to family Leguminosae (sub-family: Fabaceae), is an essential oilseed and cash crop in the tropics, subtropics, and warm temperate regions of the world [34]. And it probably derived from a hybridization event between *A. duranensis* (2n= 2x = 20, AA) and *A. ipaënsis* (2n= 2x = 20, BB) [33]. Interestingly, unlike other oilseed crops, it showcases geocarpic behavior of flowering above the ground and bearing pods below the ground [35]. As so far, many species of *Arachis* have been completed genome-wide sequence and released, including wild diploid species and tetraploid species [36–42]. These contributions have greatly promoted the research on peanut gene family mining and molecular breeding. Although

 doi:10.20944/preprints202512.1329.v1

many previous studies have been conducted on the gene family of peanut, such as WRKY [43], PIF [44], bZIP [45], and F-box [46]. However, the whole genome systematic analysis of YUCCA protein family is still insufficient.

To systematically research peanut YUC protein family, in the present study, we used bioinformatics to identify *YUC* genes of the whole genome and studied the expression pattern of the family members. The main objectives of this study include: (1) assessing the quantity, physicochemical properties, conserved domain features, gene structure, and evolutionary origins of peanut YUC family members; (2) explicating the computationally predicted expression patterns of *AhYUCs* across different peanut tissues; (3) elucidating the expression patterns of these candidate genes under multiple treatments.

2. Results

2.1. Identification of Peanut YUC Members and Chromosome Location

Utilizing the FMO–like conserved domain analysis, a total of 89 peanut YUC members were identified according to chromosome order of whole genome (Table S1 and Figure 1). Among these, 43 *AhYUCs* in AABB genome, sequentially named *AhYUC1-AhYUC43*, 25 *AdYUCs* in AA genome and 21 *AiYUCs* in BB genome, which all contained a typical FMO-like conserved domain. And then, *AdYUCs, AiYUCs, and AhYUCs* were located to 8, 8, and 15 chromosomes, excluding A04/A09, B01/B09, and Chr.04/09/11/18/19, respectively. In the AABB genome, Chr.16 harbored the maximum *AhYUCs* (n=9). For the AA and BB genomes, A06 contained the most *AdYUCs* (n=8), while B06 had the highest number of *AiYUCs* (n=6). The results indicated that most peanut *YUC* members were located preferentially toward the terminal regions of the chromosomes, with relatively fewer genes positioned in the central or medial sections.

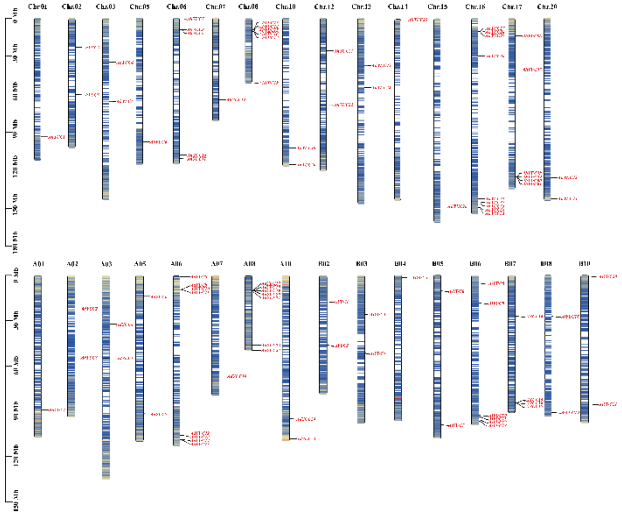

Figure 1. Chromosomes locations of peanut *YUC* members. Left ruler indicated chromosome length with Mb unit.

2.2. Physicochemical Properties and Subcellular Localization Prediction of Peanut YUC Members

Through the analysis of the physicochemical properties prediction, all peanut YUCs were identified (Table S2). The results indicated that the amino acid (aa) lengths ranged from 173–677 aa with an average length of approximately 449 aa. The relative molecular weights, isoelectric point (pI), instability index and aliphatic index ranged from 19.50–75.90 kDa, 5.56–9.48, 13.49–52.45 and 76.95–93.97, respectively. All members were hydrophilic protein. Moreover, peanut YUCs were located in various cellular structures by subcellular localization prediction. Among these, 69.66% (62/89) peanut YUCs were located in the cytoplasm, 16.85% (15/89) in the mitochondria, 8.99% (8/89) in the plasma membrane, 3.37% (3/89) in the periplasmic space, and only AhYUC16 in the chloroplasts.

 doi:10.20944/preprints202512.1329.v1

2.3. Phylogenetic Analysis of Peanut YUC Members

To describe the evolutionary relationship, peanut YUC proteins were compared with *Arabidopsis* YUC proteins (Figure 2). One hundred YUCs were classified into five clades (Clade I–IV) based on their similarity. Of these, 22 YUCs were categorized into Clade I, including 3 *AtYUCs*, 8 *AdYUCs*, 7 *AiYUCs* and 7 *AhYUCs*; 36 into Clade II with 1 *AtYUC*, 9 *AdYUCs*, 5 *AiYUCs* and 20 *AhYUCs*, 6 into Clade III with 3 *AtYUCs*, 1 *AdYUC*, 1 *AiYUC* and 2 *AhYUCs*,18 into Clade IV with 2 *AtYUCs*, 4 *AdYUCs*, 4 *AiYUCs* and 8 *AhYUCs*, and 18 into Clade V with 5 *AtYUCs*, 3 *AdYUCs*, 4 *AiYUCs* and 6 *AhYUCs*. These results indicated that peanut YUC members clustered with *Arabidopsis* homologs may share functional similarity.

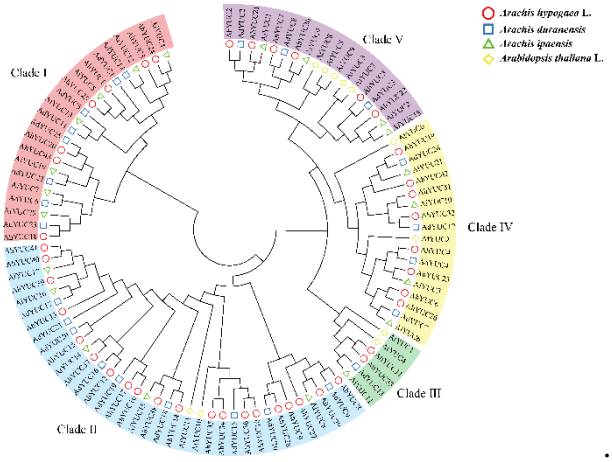

Figure 2. Phylogenetic tree of *Arachis hypogaea*, *Arachis duranensis*, *Arachis ipaensis* and *Arabidopsis thaliana*. Clade Ⅰ, Clade Ⅱ, Clade Ⅲ, Clade Ⅳ and Clade Ⅴ were indicated by red, blue, green yellow and purple, respectively.

2.4. Conserved Motifs and Gene Structural of Peanut YUC Members

A total of five conserved motifs were identified, named as motif 1–motif 5 (Table S3 and Figure 3). As expected, 95.51% (85/89) peanut YUCs contained highly representative motif 3 with 1-3 typical FMO–like domains, 88.76% (79/89) had motif 2 (NADH binding domain) and motif 4 (FMO–like domain), 74.16% (66/89) had motif 1 (indole-3-pyruvate monooxygenase domain), and 73.03% (65/89) had motif 5 with the same domain as motif 1 (Figure 3A). Of these, AiYUC8 contained the most motifs, up to 11. Conservative motif disparities could serve as a key basis for peanut YUC protein identification and categorization. Additionally, peanut YUC genes contained 0–4 UTR regions, 1–10 CDS regions and 0–9 introns (Figure 3B). Notably, 71 (79.78%) members had 1–4 UTRs, 88 (98.88%) had 1–9 introns, and AhYUC36 possessed the maximum CDSs and introns. AhYUC16 contained only one CDS, while 18 (20.22%) members lacked UTRs.

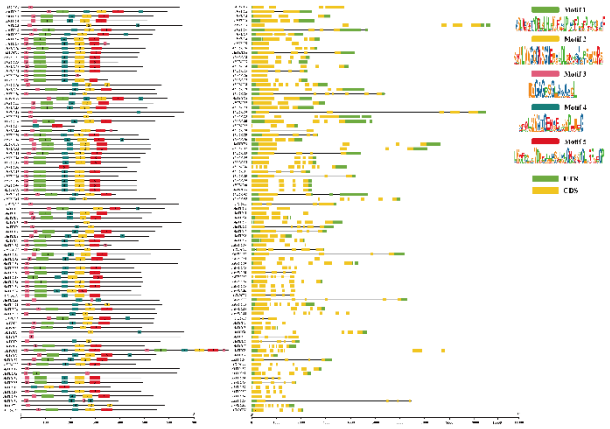

 doi:10.20944/preprints202512.1329.v1

Figure 3. Conserved motifs and gene structure of peanut *YUC* genes.

2.5. Cis-Acting Elements of Peanut YUC Genes in the Promoter Region

To predict the potential *cis*–acting elements of peanut YUC genes, a total of 3,903 elements were identified and classified into four distinct categories (Table S4 and Figure 4). The first category consisted of elements implicated in growth and developmental processes, including the WUN–motif, ARE, ERE, and as–1. The second category included elements responsive to phytohormones, such as the TCA, ABRE, and CGTCA–motif. The third category contained elements associated with light responsiveness, including the G–Box and GT1–motif. Lastly, the fourth category was composed of elements related to stress responses, such as MYB and MYC binding sites. Obviously, all *AhYUCs* were enriched with light-responsive elements, and 84.6% *AhYUCs* harbored at least one MYB/MYC binding site, implying potential roles in peanut growth and stress tolerant regulation.

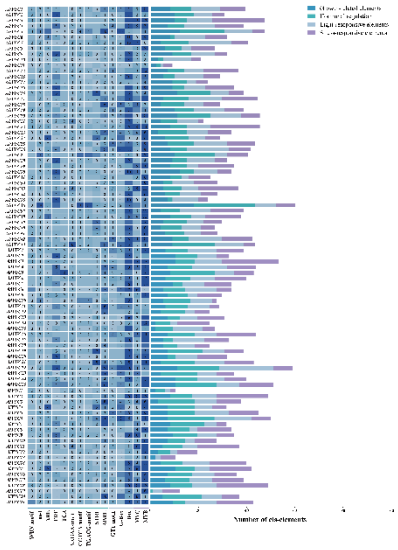

Figure 4. *Cis*–elements of promotor region in peanut *YUC* genes. Different numerical value represents the number of components involved in growth-related elements, hormone-responsive elements, light-responsive elements, stress-responsive elements.

2.6. Collinearity and Estimation of Ka/Ks Ratios of YUC Genes in Peanut

Collinearity analysis between tetraploid peanut and their diploid ancestors was conducted to further investigate the duplication events and evolutionary relationships of peanut *YUC* genes (Table S5, Table S6 and Figure 5). Of these, 34 collinear gene pairs were identified in tetraploid peanut (Figure 5A). The *Ks* values of *AhYUC* gene pairs ranged from 0.0312 to 2.5939, corresponding to duplication events spanning 159.72 millions of years ago (MYA) to 2.99 MYA (Figure 5B). However, except for *AhYUC1*/*AhYUC5*, *AhYUC5*/*AhYUC24*, and *AhYUC8*/*AhYUC28*, other gene pairs exhibited *Ka*/*Ks* < 1, indicating strong purifying selection during *AhYUCs* evolution. Subsequently, 54 collinear gene pairs were identified between AA and AABB genome, and 55 gene pairs between BB and AABB (Figure 5C). Moreover, single gene from diploid progenitor genomes often form collinear pairs with multiple tetraploid genes. Notably, a substantial number of segmental duplication events were detected in the chromosomal regions of Aradu.06/Arahy.06, Aradu.06/Arahy.16, Araip.06/Arahy.06, and Araip.06/Arahy.16. It is hypothesized that segmental duplication events have played a significant role in the evolution of peanuts.

 doi:10.20944/preprints202512.1329.v1

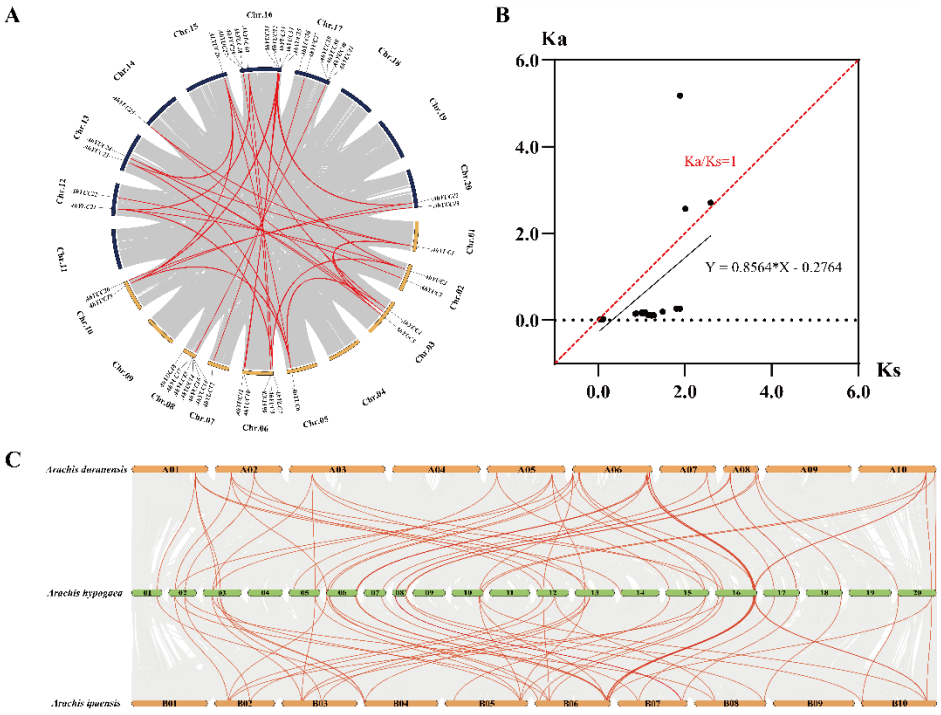

Figure 5. Collinearity plots in inter–species and intra–species, and *Ka*/*Ks* ratio of *AhYUCs* in peanut. (**A**) Red line represents the *AhYUC* genes in colinear blocks in *Arachis hypogaea*. (**B**) *Ka*/*Ks* ratio of duplicated *AhYUC* gene pairs in peanut. The black dots represent the value of *Ka*/*Ks*. The red line represent *Ka*/*Ks* = 1. (**C**) Red line represented the *AhYUC* genes in colinear blocks between *Arachis hypogaea* and its diploid progenitors.

2.7. Expression Patterns of AhYUCs in Different Tissues

To reveal the expression patterns of *AhYUCs* in different tissues, we analyzed the expression profiles of 34 tissues (Table S7 and Figure 6). Of these, 17 genes indicated that higher expression levels in different tissues. For instance, in clade I, *AhYUC18* exhibited higher expression in lateral branches, while *AhYUC43* in nodule and *AhYUC25* in seed pat. 10. In clade II, *AhYUC29* manifested widely high expression in 28 tissues, *AhYUC8* in 15 tissues, *AhYUC9* in 11 tissues and *AhYUC36* in 4 tissues. Simultaneously, *AhYUC14* and *AhYUC38* were specifically expressed in pistil, *AhYUC27* in patte 1 pod, *AhYUC28* in seed (pat. 6 and pat. 7). In clade IV, *AhYUC6* and *AhYUC26* displayed highest expression in fruit pat, while *AhYUC19*, *AhYUC23*and *AhYUC42* in perianth. In clade V, *AhYUC7* displayed highest expression in in seed pat. 10. However, *AhYUC11* and *AhYUC33* of the clade III displayed lower expression in all tissues.

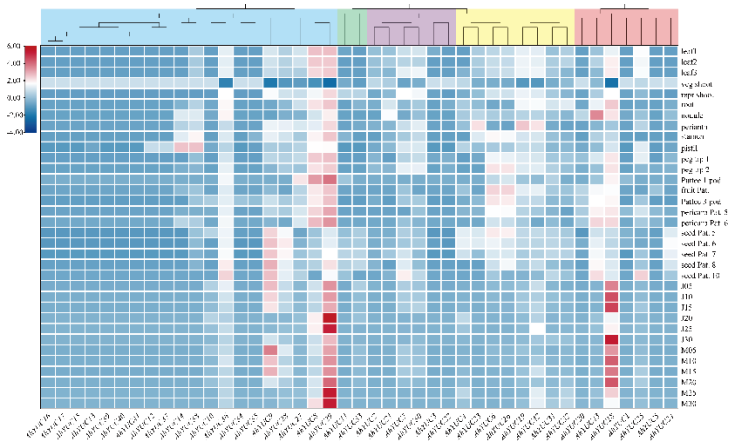

Figure 6. Expression patterns of *AhYUC* genes across various tissues and during lateral branch development. Heatmap of *AhYUC* genes expression across 22 distinct tissues and lateral branches in two genotypes. The red and blue colors indicated the higher expression and lower expression values, respectively.

 doi:10.20944/preprints202512.1329.v1

2.8. Physiological and Biochemical Differences Between Two Genotypes Genotypes and Expression Analysis of AhYUC Genes

Firstly, four physiological and biochemical indexes were measured between JH5 and M130 (Figure 7A and 7B). The results indicated that SOD, POD, APX were markedly lower in JH5 than M130 ($p < 0.01$) under drought (Figure 7A) and salt stresses (Figure 7B). In contrast, the content of MDA was significantly greater in JH5 than M130 ($p < 0.01$). Therefore, in this study, JH5 was defined as susceptible genotype, while M130 as resistance genotype. Subsequently, according to the expression profiles of 34 tissues, we selected eight *AhYUCs* to identify their expression patterns under five distinct treatments (Table S8, Figure 7C and Figure A1).

Overall, the expression levels in M130 were generally higher than in JH5 under salt stress. In contrast, *AhYUC26* and *AhYUC29* showed higher expression in JH5 after 3h of drought stress than in M130. Moreover, *AhYUC36* exhibited that irregular expression trend both two genotypes under drought stress, while *AhYUC8* under salt stress.

Under three exogenous hormones treatments, only *AhYUC29* displayed a similar expression trends across all three conditions, with significantly higher expression level in JH5 than in M130 after 6h. *AhYUC16* expression in M130 peaked at 6h or 12h then declined, while no consistent trend was observed in JH5. *AhYUC36* in M130 exhibited comparable expression dynamics, whereas its expression in JH5 displayed a parallel trend under both ABA and GA_3 treatments, with peaking at 24h. Additionally, *AhYUC6* showed a consistent up-regulation from 6h to 48h under both GA_3 and 6-BA treatments, with peaking at 48h. Other genes showed different expression profiles in response to exogenous hormone treatments.

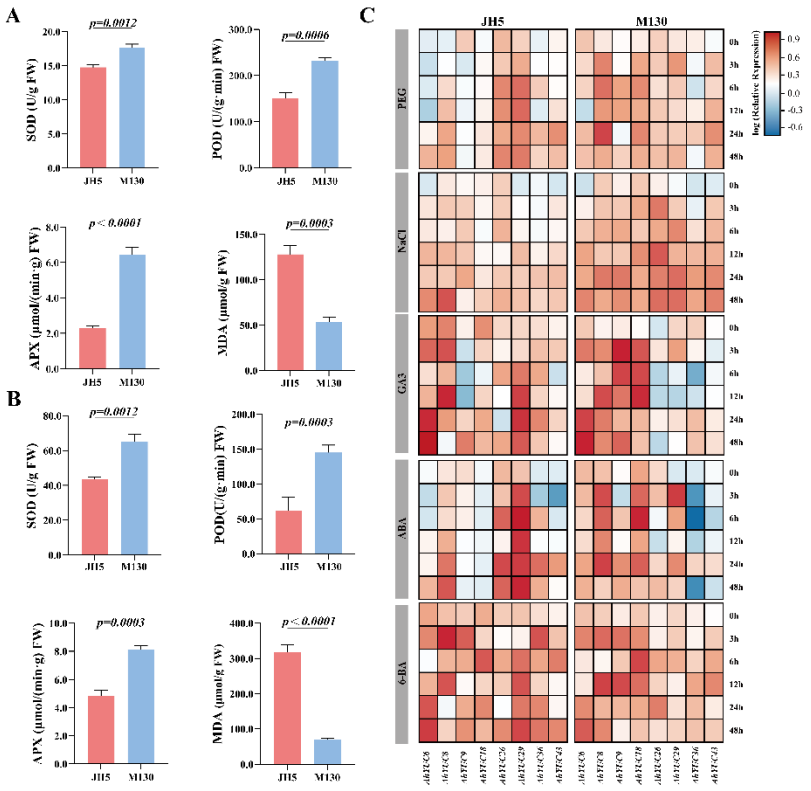

Figure 7. Physiological responses of two peanut cultivars to drought stress(A) and salt stress (B). Expression patterns analysis of *AhYUCs* by qRT-PCR of abiotic stresses and hormonal treatments (C). The X axes of the bar diagram indicated two genotypes. The Y axes of the bar diagram indicated the activities of SOD, POD, APX, and the content of MDA. Data were presented as the mean ± standard deviation (SD) with three biological repeats. The *p*-values above the bars indicate statistically significant differences between the two genotypes under the same treatment. Heatmap of *AhYUCs* gene expression under abiotic stresses and hormone treatments. The relative expression levels (log10 scale) are depicted with a color key where red and blue denote up-regulation and down-regulation, respectively, compared to the 0 h control. The samples include two genotypes (JH5, M130)

 doi:10.20944/preprints202512.1329.v1

across a time course after soil drench with PEG and NaCl, and foliar spraying with GA_3, ABA, and 6-BA on peanut plants.

3. Discussion

YUC as a key rate-limiting enzymes for IAA biosynthesis, widely involved into plant growth and development and abiotic stresses. From non-seed vascular plants to vascular plants, its proteins have diverged to ensure correct domain specialization, and there are different in quantity [14]. To date, previous studies have been extensively identified in numerous higher plants by genome-wide phylogenetic analysis, while such studies remain scarce for leguminous crops. For example, alfalfa contained 12 *MsYUCs* (*Medicago sativa*) and 15 *MtYUCs* (*Medicago truncatula*) [21,47], and soybean (*Glycine max*) had 22 *GmYUCs* [20,48]. Compared with the number of YUC family genes in other leguminous crops, in our study, we identified 43 *AhYUCs* in allotetraploid peanut (*A. hypogaea*), along with 25 *AdYUCs* and 21 *AiYUCs* in its diploid progenitors *A. duranensis* and *A. ipaensis*, respectively. Obviously, the members of peanut diploid was similar to soybean, while more than alfalfa diploid. However, allotetraploid peanut showed higher number. This difference in gene number may be attributed to the allotetraploid nature of cultivated peanut, which originated from the hybridization and genome segment duplication of *A. duranensis* and *A. ipaensis* [36]. The combination of the two diploid genomes likely contributed to the expansion of the AhYUC family, providing a broader genetic basis for regulation in response to diverse environmental cues and developmental processes.

The functional diversity of *YUC* genes is often closely associated with their differential regulatory elements. In previous studies, the promoter of *YUC* gene contained many types of *cis* -elements, mainly light-responsive, ABA-responsive, gibberellin-responsive and drought-inducing elements [49]. In the present study, our results revealed an enrichment of diverse *cis*–acting elements related to growth and development, light responsiveness, phytohormone response, and stress responses, including ARE, G-box, ERE, MYB, BOX, and TCA-elements etc. It suggested that *AhYUCs* may be subject to complex transcriptional control, thereby enabling their involvement in a wide range of physiological and biochemical processes in peanut. Of these elements, a total of 597 MYB binding sites, as the most abundance *cis* elements, were identified in peanut YUC members in our study. As we know, MYB elements can be bound by MYB transcription factors [50]. For now, there is no evidence that *MYB* transcription factor can be directly regulated *YUC* gene expression by binding to *MYB cis*–element of YUC promoter region. However, previous study have proven that *MYB112* physically interacts with PIF4 to indirectly enhance the transcription of PIF4 target gene *YUC8* involved in the auxin pathway, such as, resulted in high temperature–induced hypocotyl elongation in *Arabidopsis* [51,52]. Thus, whether MYB transcription factors directly regulate *YUC* genes remains to be determined in peanut and represents a worthwhile scientific question. Additionally, the G-box as a *cis*-acting DNA regulatory element found in plant genome, and the interaction with regulatory genes can be achieved the expression of *YUC* genes [53]. For example, *AtPIF4* bound to the G-box in the *AtYUC8* promoter, promoted auxin biosynthesis and drove hypocotyl elongation [54]. MYC transcription factors specifically bound to G-box of *YUC8* and *YUC9* promoters, triggered IAA formation and thereby reduced two-spotted spider mite damage to tobacco leaves [55]. In our study, 188 G-box elements of peanut *YUC* genes were identified, implying *AhYUCs* potential regulation by upstream factors and roles in light and biotic stress responses. Taken together, elucidating the direct or indirect interaction modes between various regulation factors and *YUC* promoters is crucial for understanding the intricate spatiotemporal control of auxin biosynthesis.

When analyzing the expression profile of *AhYUCs*, we found that *AhYUC* genes were highly expressed in specific tissues or developmental stages. Notably, several *AhYUCs* exhibited high expression in reproductive tissues such as flowers and seeds, suggesting their involvement in pollen development, lateral organ morphogenesis and seed development. Such as *AhYUC9* and *AhYUC36*, belonging to clade II, exhibited high expression during seed development or in specific seed tissues (seed Pat. 10). Similarly, *AtYUC10* and *AtYUC11* in the same clade, were confirmed that regulated seed size and embryo development, respectively [56,57]. This similarity in expression patterns

 doi:10.20944/preprints202512.1329.v1

suggested that *AhYUC9* and *AhYUC36* may have conserved functions in peanut seed development. Furthermore, other *AhYUCs* in clade II had high expression across various vegetative and reproductive organs, implied that their potential involvement in plant growth and development processes. In addition, *AhYUC6* and *AhYUC26* were sorted into clade IV with some *AtYUCs*, including *AtYUC2* and *AtYUC6*. Previous study showed that, the expression of *YUC2* and *YUC6* in diploid microsporocytes was essential for the early stages of pollen development [58], and SPOROCYTELESS might regulated auxin homeostasis by suppressing the transcription of *YUC2* and *YUC6*, thereby participating in lateral organ morphogenesis [59]. In our study, *AhYUC6* and *AhYUC26* showed high expression in peg tip, fruit, pericarp and seed, and *AhYUC29* exhibited high expression in lateral branches, which speculated that they were involved in the regulation of different stages of peanut pod, seed and lateral branches development.

The response of *AhYUCs* to abiotic stress (drought and salt) and exogenous hormones (GA_3, ABA and 6-BA) further highlighted the complexity of their regulatory networks. In our study, Obviously, *AhYUC29* had a significant change trend after 3h or 6h between JH5 and M130 under NaCl and PEG6000 stresses. The similar expression trend of *AhYUC29* across all three hormone treatments, with higher expression in JH5 at 6h. Thus, we suggested a conserved regulatory mechanism for this gene in response to different stresses and hormonal cues, although its specific role in distinct genotype remains unclear. The irregular expression trends of some *AhYUCs*, such as *AhYUC36* under drought stress and *AhYUC8* under salt stress, in both genotypes, suggested that the regulation of auxin biosynthesis under abiotic stress is complex and may involve feedback mechanisms or cross-talk with other signaling pathways. Previous studies in *Arabidopsis* has demonstrated that *YUCCA7* was upregulated under drought stress in an ABA-dependent manner, and its overexpression enhanced drought resistance primarily through promoting root growth. [60], overexpression of *PagYUC6a* in poplar promoted root development via increased auxin levels, leading to enhanced salt tolerance. [61]. The peaked expression of *AhYUC16* at specific time points (6h, 12h, or 24h) in M130 indicated that these genes might be involved in short-term or delayed hormonal responses, which could be important for fine-tuning auxin levels during stress adaptation or developmental transitions. The consistent up-regulation of *AhYUC6* from 6h to 48h under GA_3 and 6-BA treatments in both genotypes, suggested a role in mediating the synergistic effects of gibberellins and cytokinins with auxin, possibly in promoting cell elongation or division under favorable conditions [62]. The differential expression patterns of other *AhYUCs* in response to hormones imply that individual *YUC* genes may be subject to distinct regulatory mechanisms, allowing the plant to integrate multiple hormonal signals to precisely control auxin biosynthesis in a context-dependent manner.

Collectively, the integration of phylogenetic, tissue-specific, and stress/hormone-induced expression analyses of the *AhYUC* family provides a comprehensive framework for understanding their roles in peanut development and stress tolerance. The expansion of the *AhYUC* family, their conserved phylogenetic relationships, and dynamic expression patterns underscore their functional diversity and importance in auxin-mediated processes.

4. Materials and Methods

4.1. Genome-Wide Identification and Chromosome Localization

The genomic data for *A. duranensis*, *A. ipaensis*, and the cv. Tifrunner were retrieved from the PeanutBase database. (http://peanutbase.org/, accessed on 12 October 2024). The HMMER v3.3.2 software (http://hmmer.org/, accessed on 12 October 2024) was employed to identify YUC protein sequences. This was done using the FMO-like conserved domain (PF00743) as the query model, applying a significance threshold of E-value ≤ 1×10^{-10}. Once redundant sequences were excluded, potential sequences were submitted to the SMART (http://smart.embl-heidelberg.de/, accessed on 12 October 2024), Pfam database (http://pfam-legacy.xfam. org/, accessed on 12 October 2024), and CDD (http://www.ncbi.nlm.nih.gov/Structure/cdd/wrpsb.cgi, accessed on 12 October 2024) databases, in

 doi:10.20944/preprints202512.1329.v1

order to validate whether the retrieved protein sequences incorporated the appropriate conserved domains. Family members were labeled according to their sequential appearance on the respective genomic chromosomes, ranging from *AhYUC1* to *AhYUCn*, *AdYUC1* to *AdYUCn* and *AiYUC1* to *AiYUCn*. The chromosomal location diagram was generated with MapChart 2.32 [63], using the physical positions of *AhYUCs*, *AdYUCs*, and *AiYUCs* from their respective reference genomes.

4.2. Physicochemical Properties, Phylogenetic Tree and Gene Structure Analysis

The physicochemical properties of the entire gene family were analyzed using the ExPASy server (http://www.expasy.org/tools/protparam, accessed on 26 October 2024). [64], predicting key properties including amino acid count, molecular weight, isoelectric point (pI), instability index, aliphatic index, and grand average of hydropathicity. Subcellular localization was predicted using CELLO v.2.5 (http://cello.life.nctu.edu.tw/, accessed on 26 October 2024). Protein sequences of AtYUC were downloaded from NCBI (https://www.ncbi.nlm.nih.gov/, accessed on 26 October 2024). Subsequently, a phylogenetic analysis of *AhYUCs*, *AdYUCs*, *AiYUCs* and *AtYUCs* was performed using MEGA X (Bootstrap = 1000 replicates) [65]. Conserved protein motifs were identified using the MEME suite; in parallel, exon-intron gene structures were also predicted (http://meme-suite.org/tools/meme, accessed on 26 October 2024), [66] and the online platform Gene Structure Display Server (GSDS) 2.0 (http://gsds.gao-lab.org/, accessed on 26 October 2024) [67].

4.3. Prediction of Cis–Acting Elements in the Promoter Region

The 2,000 bp promoter regions upstream of the *AhYUCs*, *AdYUCs*, and *AiYUCs* were analyzed for *cis*-acting regulatory elements. These predictions were performed using the PlantCARE database (http://bioinformatics.psb.ugent.be/webtools/plantcare/html/, accessed on 17 November 2024), and subsequently visualized in a comprehensive cis-acting element map constructed with GSDS 2.0. [67].

4.4. Collinearity and Estimation of Ka/Ks Ratios Analysis

Gene collinearity analysis was conducted with the one-step MCScanX module in TBtools (v1.132, E-value < 1×10^{-5}). Subsequently, the Ka/Ks ratios for the identified syntenic gene pairs were calculated using the built-in "Simple Ka/Ks Calculator" in TBtools. [68–70]. These tools enhanced the clarity of evolutionary interpretation by enabling the estimation of duplication event divergence times, calculated as $T = Ks/(2\lambda)$, with the neutral substitution rate λ for peanut set at 8.12×10^{-9} [35].

4.5. In Silico Expression Analysis of AhYUC Genes in Thirty-Fourt Tissues

To investigate the tissue-specific expression patterns of AhYUC genes, we analyzed data quantified in Fragments Per Kilobase of exon per Million mapped fragments (FPKM). Transcriptomic data for various tissues and first lateral branch development (BioProject: PRJNA675413) [71] were obtained from the PeanutBase Expression Atlas and the NCBI SRA. These expression data (FPKM) were then normalized by log2(FPKM+1) transformation for downstream analysis. Subsequent normalization was performed using z-score method, denoted by the equation $(\sum(x^2)-(\sum x)^2/n)/n$. Within this equation, 'x' represents the raw value, while 'n' denotes the number of data points. To visualize gene expression, a heatmap was generated using TBtools II [69].

4.6. Plant Materials, Growth Conditions and Treatments

To further investigate the expression patterns of *AhYUCs* in response to abiotic stress and exogenous hormones, two genotypes (JH5 and M130) featuring distinct plant types characteristics were selected for analysis [72]. They were grown under rigorously controlled environmental conditions within a climatically-controlled chamber, maintained at a stable temperature of 25 °C. Furthermore, they were subjected to a circadian rhythm consisting of 16 h of light succeeded by 8 h of darkness.

 doi:10.20944/preprints202512.1329.v1

For the physiological indices assay, twelve-day-old seedlings (at the three-leaf stage) were subjected to two sustained stress treatments to confirm the fundamental stress tolerance difference at the physiological level. The salt stress group was treated by irrigating with 250 mM NaCl solution, while the drought stress group underwent natural drought treatment by withholding water. Leaf fresh samples were collected 24 hours after salt treatment and 16 days after the initiation of drought stress, respectively. The activities of antioxidant enzymes and the content of malondialdehyde were determined using commercial assay kits (Suzhou Grace Biotechnology Co., Ltd., Suzhou, China) following the manufacturer's protocols. Specifically, the activity of superoxide dismutase (SOD) was measured using the WST-8 method (Kit No. G0101W), the activity of peroxidase (POD) was determined using the guaiacol method (Kit No. G0107W), and the activity of ascorbate peroxidase (APX) was assayed (Kit No. G0203W). The malondialdehyde (MDA) content was determined via the thiobarbituric acid (TBA) method (Kit No. G0109W). The absorbance for each assay was recorded using a Multimode reader (TECAN, Männedorf, Switzerland).

4.7. Hormone and Abiotic Stress Treatments for qRT-PCR Analysis

To investigate the dynamic expression profiles of *AhYUC* genes in response to various signals, twelve-day-old seedlings (at the three-leaf stage) of JH5 and M130 were subjected to five different treatments with application methods tailored to the nature of each elicitor. To simulate direct soil environmental stresses, root irrigation was performed using 15% (w/v) PEG-6000 solution to mimic osmotic stress and 250 mM NaCl solution for salt stress. In contrast, to assess leaf responses to specific plant hormones, foliar spray was applied with solutions of 200 μmol/L abscisic acid (ABA), 200 μmol/L gibberellin A_3 (GA_3), or 15 mg/L 6-benzylaminopurine (6-BA) using an atomizer at 0.2 MPa nozzle pressure. For foliar applications, the nozzle was positioned 20 cm above the canopy, delivering approximately 5 mL per plant until leaves were fully wetted without runoff. The third trifoliate leaves were sampled at 0 (control), 3, 6, 12, 24, and 48 hours post-treatment (hpt), with n = 5 biologically independent plants collected per time point. All samples were excised and immediately flash-frozen in liquid nitrogen within 15 seconds, then stored at -80°C for subsequent RNA extraction.

4.8. RNA Extracted and qRT–PCR Analysis

Following extraction with the FastPure Universal Plant Total RNA Isolation Kit (Vazyme, Nanjing, China). RNA samples were checked for integrity via Gel electrophoresis and quantified for concentration using a NanoDrop™ One (ThermoFisher, Waltham, USA). First-strand cDNA synthetization was performed using the Hiscript II QRT SuperMix for qPCR (Vazyme, Nanjing, China). Gene-specific primers for qRT-PCR were designed based on the CDS sequences using Primer Premier 5 software, with their specificity verified by BLAST against the NCBI database (Table S9). PCR amplification system and procedure were conducted following the protocol described previously [73]. The relative expression of candidate genes was calculated utilizing $2^{-\Delta\Delta Ct}$ method [74]. GraphPad Prism 8.0 software was used for Student's *t*-test ($p < 0.01$) and correlation analysis ($p < 0.01$).

Supplementary Materials: The following supporting information can be downloaded at the website of this paper posted on Preprints.org. Table S1: Sequences and physical location of the *AhYUCs*, *AdYUCs* and *AiYUCs*; Table S2: Prediction of physicochemical properties of *AhYUCs*, *AdYUCs*, and *AiYUCs*; Table S3: Motif sequence of *YUCCA* gene family in peanut; Table S4: *Cis*-element analysis of *AhYUCs*, *AdYUCs* and *AiYUCs* gene promoters; Table S5: Syntenic relationships between *Arachis hypogaea* and *Arachis duranensis*, *Arachis ipaensis*; Table S6: *Ka*/*Ks* analysis and years of genetic evolution; Table S7: Published transcriptome data of the various tissues and lateral branch development transcriptome expression in cultivated peanuts; Table S8: The relative expression data of nine *AhYUC* genes; Table S9: Sequences of the primers used in this study.

Author Contributions: Conceptualization, X.Y.; methodology, X.Y.; software, C.L. and G.L.; validation, C.L. and G.T.; formal analysis, X.Y.; investigation, C.L., S.L., and J.W.; resources, X.Y. and C.Y.C.; data curation, C.L. and

 doi:10.20944/preprints202512.1329.v1

Y.Q.; writing-original draft preparation, C.L.; writing-review and editing, X.Y. and C.Y.C.; visualization, X.Y.; supervision, X.Y.; project administration, X.Y.; funding acquisition, X.Y. All authors have read and agreed to the published version of the manuscript.

Funding: This research was supported by the Hebei Agriculture Research System (Grant No. HBCT20240201); the Central Guidance on Local Science and Technology Development Fund of Hebei Province (Grant No. 246Z2910G); the S&T Program of Hebei (Grant No. 252N7501D and 24466301D); the Science Research Project of Hebei Education Department (Grant No. YJZ2024001); the Top Young Talents Support Program of Hebei Province (Grant No. 0602015); the State Key Laboratory of North China for Crop Improvement and Regulation (Grant No. NCCIR2022zz–6).

Data Availability Statement: Transcriptome data are available in the NCBI with accession number PRJNA675413.

Conflicts of Interest: The authors declare no conflicts of interest.

Appendix A

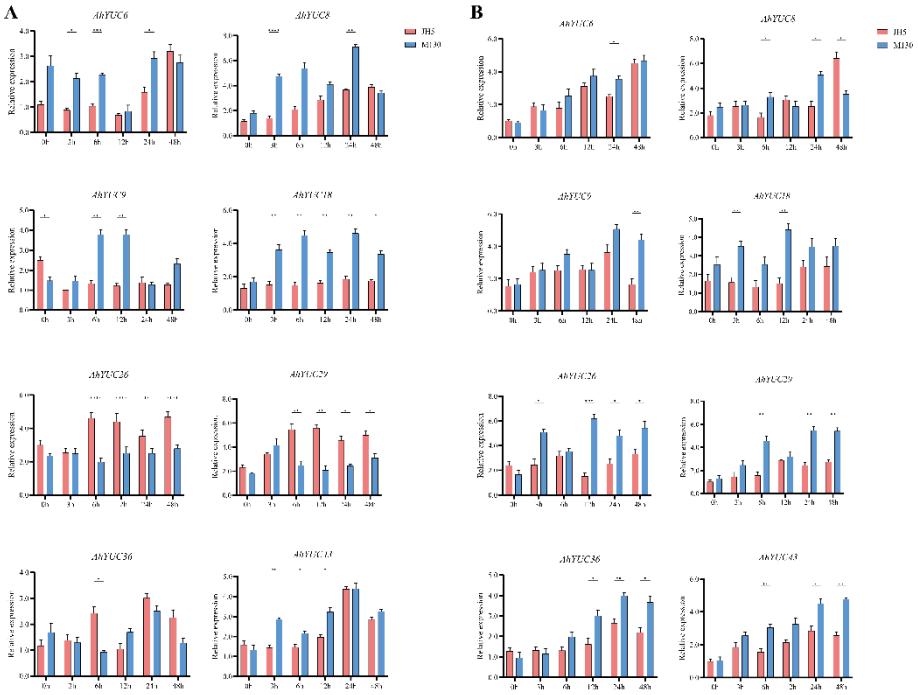

Figure A1. (A) Expression patterns of *AhYUCs* by qRT-PCR of drought stress, (B) Expression patterns of *AhYUCs* by qRT-PCR of salt stress. The red bar diagram represented expression pattern during the time points after abiotic stress treatment of JH5. The blue bar diagram showed expression pattern during the time points after abiotic stress treatment of M130.. The X axes of the bar diagram indicated times after PEG6000 and NaCl stress. The Y axes of the bar diagram indicated the relative expression levels of DEGs, respectively. The asterisks denote levels of statistical significance: * $p < 0.05$, ** $p < 0.01$, *** $p < 0.001$, **** $p < 0.0001$.

References

1. Jodder, J. miRNA-mediated regulation of auxin signaling pathway during plant development and stress responses. *J Biosci*. **2020**, *45*,91.
2. Casanova-Sáez, R.; Voß, U. Auxin metabolism controls developmental decisions in Land plants. *Trends Plant Sci*. **2019**, *24*, 741–754.
3. Wang, P.; Duan, Y.; Quan, R.; Feng, M.; Ren, J.; Tang, Y.; Qing, M.; Xie, K.; Guo, W.; Wu, X. *CsTCP14-CsIAA4* module-mediated repression of auxin signaling regulates citrus somatic embryogenesis. *New Phytol*. **2025**, *246*, 567-580.
4. García-Gómez, ML.; Garay-Arroyo, A.; García-Ponce, B.; Sánchez, MP.; Álvarez-Buylla, ER. Hormonal

 doi:10.20944/preprints202512.1329.v1

regulation of stem cell proliferation at the *Arabidopsis thaliana* root stem cell niche. *Front Plant Sci*. **2021**, *12*, 628491.

5. Tsukaya, H.; Kozuka, T.; Kim, GT. Genetic control of petiole length in *Arabidopsis thaliana*. *Plant Cell Physiol*. **2002**, *43*, 1221-1228.
6. Ahmad, S.; Lu, C.; Wu, J.; Wei, Y.; Gao, J.; Jin, J.; Zheng, C.; Zhu, G.; Yang, F. Transcriptional Cascade in the Regulation of Flowering in the Bamboo Orchid *Arundina graminifolia. Biomolecules* **2021**, *11*, 771.
7. Simonini, S.; Østergaard, L. Female reproductive organ formation: A multitasking endeavor. *Curr Top Dev Biol*. **2019**, *131*, 337-371.
8. Li, S.; Zhao, Y.; Wu, P.; Grierson, D.; Gao, L. Ripening and rot: How ripening processes influence disease susceptibility in fleshy fruits. *J Integr Plant Biol*. **2024**, *66*, 1831-1863.
9. Park CM. Auxin homeostasis in plant stress adaptation response. *Plant Signal Behav*. **2007**, *2*, 306-307.
10. Luo, P.; Di, D.-W. Precise Regulation of the TAA1/TAR-YUCCA Auxin Biosynthesis Pathway in Plants. *Int. J. Mol. Sci*. **2023**, *24*, 8514.
11. Wu, H.; Yang, J.; Shen, P.; Li, Q.; Wu, W.; Jiang, X.; Qin, L.; Huang, J.; Cao, X.; Qi, F. High-Level production of Indole-3-acetic Acid in the metabolically engineered *Escherichia coli*. *J Agric Food Chem*. **2021**, *69*, 1916-1924.
12. Won, C.; Shen, X.; Mashiguchi, K.; Zheng, Z.; Dai, X.; Cheng, Y.; Kasahara, H.; Kamiya, Y.; Chory, J.; Zhao, Y. Conversion of tryptophan to indole-3-acetic acid by TRYPTOPHAN AMINOTRANSFERASES OF *ARABIDOPSIS* and YUCCAs in *Arabidopsis*. *Proc. Natl. Acad. Sci. USA*. **2011**, *108*, 18518-18523.
13. Turnaev, I.I.; Gunbin, K.V.; Suslov, V.V.; Akberdin, I.R.; Kolchanov, N.A.; Afonnikov, D.A. The phylogeny of class B Flavoprotein Monooxygenases and the origin of the YUCCA protein family. Plants. **2020**, 9, 1092.
14. Cao, X.; Yang, H.; Shang, C.; Ma, S.; Liu, L.; Cheng, J. The Roles of Auxin Biosynthesis *YUCCA* Gene Family in Plants. *Int. J. Mol. Sci.* **2019**, *20*, 6343.
15. Vijayanathan, M.;;Faryad, A.; Abeywickrama, T.D.; Christensen, J.M.; Neilsonx, E.H,J. The auxin gatekeepers: Evolution and diversification of the YUCCA family. *Plant J.* **2025**, *124*, e70563.
16. Cheng, Y.; Dai, X.; Zhao, Y. Auxin biosynthesis by the YUCCA flavin monooxygenases controls the formation of floral organs and vascular tissues in *Arabidopsis*. *Genes Dev*. **2006**, *20*, 1790-1799.
17. Yamamoto, Y.; Kamiya, N.; Morinaka, Y.; Matsuoka, M.; Sazuka, T. Auxin biosynthesis by the *YUCCA* genes in rice. *Plant Physiol*. **2007**, *143*, 1362-1371.
18. Li, W.; Zhao, X.; Zhang, X. Genome-wide analysis and expression patterns of the *YUCCA* genes in Maize. *J Genet Genomics*. **2015**, *42*, 707-710.
19. Yang, Y.; Xu, T.; Wang, H.; Feng, D. Genome-wide identification and expression analysis of the *TaYUCCA* gene family in wheat. *Mol Biol Rep*. **2021**, *48*, 1269-1279.
20. Wang, Y., Liu, H., Wang, S., Li, H. Genome-wide identification and expression analysis of the *YUCCA* gene family in soybean (*Glycine max* L.). *Plant Growth Regul*. 2017, 81, 265-275.
21. Shao, A.; Fan, S.; Xu, X.; Wang, W.; Fu, J. Identification and evolution analysis of *YUCCA* genes of *Medicago sativa* and *Medicago truncatula* and their expression profiles under abiotic stress. *Front Plant Sci*. **2023**, *14*, 1268027.
22. Yan, S.; Che, G.; Ding, L.; Chen, Z.; Liu, X.; Wang, H.; Zhao, W.; Ning, K.; Zhao, J.; Tesfamichael, K.; et al. Different cucumber *CsYUC* genes regulate response to abiotic stresses and flower development. *Sci Rep*. **2016**, *6*, 20760.
23. Qin, M.; Wang, J.; Zhang, T.; Hu, X.; Liu, R.; Gao, T.; Zhao, S.; Yuan, Y.; Zheng, J.; Wang, Z.; et al. Genome-wide identification and analysis on *YUCCA* gene family in *Isatis indigotica* fort. And *IiYUCCA6-1* functional exploration. Int. J. Mol. Sci. **2020**, 21, 2188.
24. Luo, W.; Xiao, N.; Wu, F.; Mo, B.; Kong, W.; Yu, Y. Genome-Wide Identification and Characterization of *YUCCA* Gene Family in *Mikania micrantha*. Int. J. Mol. Sci. **2022**, 23, 13037.
25. Wang, X.; Chen, B.; Ma, C.; Qiao, K.; Li, Z.; Wang, J.; Peng, R.; Fan, S.; Ma, Q. Systematical characterization of *YUCCA* gene family in five cotton species, and potential functions of *YUCCA22* gene in drought resistance of cotton. *Ind Crops Prod*. **2021**, *162*, 113290.
26. Wu, R.; Chen, J.; Lin, Y.; Jia, Q.; Guo, Y.; Liu, J.; Yan, Q.; Xue, C.; Chen, X.; Yuan, X. Genome-wide identification, expression analysis, and potential roles under abiotic stress of the *YUCCA* gene family in

 doi:10.20944/preprints202512.1329.v1

Mung bean (*Vigna radiata* L.). Int. J. Mol. Sci. **2023**, 24, 1603.

27. Zhao, Y.; Christensen, SK.; Fankhauser, C.; Cashman, JR.; Cohen, JD.; Weigel, D.; Chory, J. A role for flavin monooxygenase-like enzymes in auxin biosynthesis. *Science*. **2001**, *291*, 306-309.
28. Chen, Q.; Dai, X.; De-Paoli, H.; Cheng, Y.; Takebayashi, Y.; Kasahara, H.; Kamiya, Y.; Zhao, Y. Auxin overproduction in shoots cannot rescue auxin deficiencies in *Arabidopsis* roots. *Plant Cell Physiol*. **2014**, *55*, 1072-1079.
29. Woo, YM.; Park, HJ.; Su'udi, M.; Yang, JI.; Park, JJ.; Back, K.; Pake, YM.; An, G. *Constitutively wilted 1*, a member of the rice *YUCCA* gene family, is required for maintaining water homeostasis and an appropriate root to shoot ratio. *Plant Mol Biol*. **2007**, *65*, 125-136.
30. Sun, J.; Qi, L.; Li, Y.; Chu, J.; Li, C. PIF4-mediated activation of *YUCCA8* expression integrates temperature into the auxin pathway in regulating arabidopsis hypocotyl growth. *PLoS Genet*. **2012**, *8*, e1002594.
31. Lee, M.; Jung, J.; Han, D.; Seo, P.; Park, W.; Park, C. Activation of a flavin monooxygenase gene *YUCCA7* enhances drought resistance in *Arabidopsis*. *Planta*. **2012**, *235*, 923-38.
32. Liu, G.; Gao, S.; Tian, H.; Wu, W.; Robert, HS.; Ding, Z. Local transcriptional control of YUCCA regulates auxin promoted root-growth inhibition in response to aluminium stress in *Arabidopsis*. *PLoS Genet*. **2016**, *12*, e1006360.
33. Halward, T.; Stalker, T.; LaRue, E.; Kochert, G. Use of single-primer DNA amplifications in genetic studies of peanut (*Arachis hypogaea* L.). *Plant Mol Biol*. **1992**, *18*, 315-325.
34. Gong, F.; Li, Z.; Sun, X.; Fan, Y.; Liu, Y.; Dang, Y.; Li, H.; Zhang, X.; Ma, X.; Li, Z.; et al. Comprehensive analysis and selection of high oleic peanut varieties in China: A study on agronomic, yield, and quality traits. *Oil Crop Science*. **2024**, *9*, 265-274.
35. Peng, Z.; Jia, K.; Meng, J.; Wang, J.; Zhang, J.; Li, X.; Wan, S. Transcriptome profiling of aerial and subterranean peanut pod development. *Sci Data*. **2024**, *11*, 364.
36. Bertioli, D.J.; Cannon, S.B.; Froenicke, L.; Huang, G.; Farmer, A.D.; Cannon, E.K.; Liu, X.; Gao, D.; Clevenger, J.; Dash, S.; et al. The genome sequences of *Arachis duranensis* and *Arachis ipaensis*, the diploid ancestors of cultivated peanut. *Nat. Genet*. **2016**, *48*, 438–446.
37. Yin, D.; Ji, C.; Ma, X.; Li, H.; Zhang, W.; Li, S.; Liu, F.; Zhao, K.; Li, F.; Li, K.; et al. Genome of an allotetraploid wild peanut *Arachis monticola*: a de novo assembly. *Gigascience*. **2018**, *7*, giy066.
38. Bertioli, D.J.; Jenkins, J.; Clevenger, J.; Dudchenko, O.; Gao, D.; Seijo, G.; Leal-Bertioli, S.C.M.; Ren, L.; Farmer, A.D.; Pandey, M.K.; et al. The genome sequence of segmental allotetraploid peanut *Arachis hypogaea*. *Nat. Genet*. **2019**, *51*, 877–884.
39. Zhuang, W.; Chen, H.; Yang, M.; Wang, J.; Pandey, M.K.; Zhang, C.; Chang, W.C.; Zhang, L.; Zhang, X.; Tang, R.; et al. The genome of cultivated peanut provides insight into legume karyotypes, polyploid evolution and crop domestication. *Nat. Genet*. **2019**, *51*, 865–876.
40. Chen, X.; Lu, Q.; Liu, H.; Zhang, J.; Hong, Y.; Lan, H.; Li, H.; Wang, J.; Liu, H.; Li, S.; et al. Sequencing of cultivated peanut, *Arachis hypogaea*, yields insights into genome evolution and oil improvement. *Mol. Plant*. **2019**, 12, 920–934.
41. Wang, X.; Sun, Z.; Qi, F.; Zhou, Z.; Du, P.; Shi, L.; Dong, W.; Huang, B.; Han, S.; Pavan, S.; et al. A telomere-to-telomere genome assembly of the cultivated peanut. *Mol Plant*. **2025**, *6*, 5-8.
42. Zhao, K.; Xue, H.; Li, G.; Chitikineni, A.; Fan, Y.; Cao, Z.; Dong, X.; Lu, H.; Zhao, K.; et al. Pangenome analysis reveals structural variation associated with seed size and weight traits in peanut. *Nat. Genet*. **2025**, *57*, 1250-1261.
43. Zhao, N.; He, M.; Li, L.; Cui, S.; Hou, M.; Wang, L.; Mu, G.; Liu, L.; Yang, X. Identification and expression analysis of WRKY gene family under drought stress in peanut (*Arachis hypogaea* L.). *PLoS ONE* **2020**, *15*, e0231396.
44. Wang, X.; Liu, Y.; Huai, D.; Chen, Y.; Jiang, Y.; Ding, Y.; Kang, Y.; Wang, Z.; Yan, L.; Jiang, H.; et al. Genome-wide identification of peanut PIF family genes and their potential roles in early pod development. *Gene*. **2021**, *781*, 145539.
45. Wang, Z.; Yan, L.; Wan, L.; Huai, D.; Kang, Y.; Shi, L.; Jiang, H.; Lei, Y.; Liao, B. Genome-wide systematic characterization of bZIP transcription factors and their expression profiles during seed development and in response to salt stress in peanut. *BMC Genomics*. **2019**, *20*, 51.

46. Li, C.; Guo, L.; Wang, W.; Miao, P.; Mu, G.; Chen, C.Y.; Meng, C.; Yang, X. Genome-Wide Identification, Characterization and Expression Profile of F-Box Protein Family Genes Shed Light on Lateral Branch Development in Cultivated Peanut (*Arachis hypogaea* L.). *Horticulturae.* **2024**, *10*, 255.
47. Shen, L.; Yi, C.; Liu, Y.; Han, F.; Feng, J. Two complete telomere-to-telomere genome assemblies of Medicago reveal the landscape and evolution of its centromeres. *Mol Plant*. **2025**, *18*, 1409-1412.
48. Liang, S.; Duan, Z.; He, X.; Yang, X.; Yuan, Y.; Liang, Q.; Pan, Y.; Zhou, G.; Zhang, M.; Liu, S., et al. Natural variation in GmSW17 controls seed size in soybean. *Nat Commun.* **2024**, *15*, 7417.
49. Zhang, K.; Zhang, J.; Cui, C.; Chai, L.; Zheng, B.; Jiang, J.; Li, H.; Tu, J. Genome-wide identification and expression profiling of the *YUCCA* gene family in *Brassica napus*. *Oil Crop Sci.* **2022**, *7*, 103-111.
50. Ma, R.; Liu, B.; Geng, X.; Ding, X.; Yan, N.; Wang, W.; Sun, X.; Zheng, C. Biological function and stress response mechanism of MYB transcription factor family genes. *J Plant Growth Regul.* **2023,** *42* , 83-95 .
51. Cai, Y.; Liu, Y.; Fan, Y.; Li, X.; Yang, M.; Xu, D.; Wang, H.; Deng, X.; Li, J. MYB112 connects light and circadian clock signals to promote hypocotyl elongation in *Arabidopsis*. *Plant Cell.* **2023,** *35*, 3485-3503.
52. Sun, J.; Qi, L.; Li, Y.; Chu, J.; Li, C. PIF4–mediated activation of *YUCCA8* expression integrates temperature into the auxin pathway in regulating *Arabidopsis* hypocotyl growth. *PLoS Genet.* **2012**, *8*, e1002594.
53. Menkens, A.; Schindler, U., Cashmore, A. The G-box: a ubiquitous regulatory DNA element in plants bound by the GBF family of bZIP proteins. *Trends Biochem Sci*, **1995**, *20,* 506–510.
54. Woude, L.; Perrella, G.; Snoek, B.; Hoogdalem, M.; Novák, O.; Verk, M.; Kooten, H.; Zorn, L.; Tonckens, R., Dongus, J.; et al. HISTONE DEACETYLASE 9 stimulates auxin-dependent thermomorphogenesis in *Arabidopsis* thaliana by mediating H2A.Z depletion. *Proc Natl Acad Sci U S A*. **2019**, *116*, 25343–25354.
55. Pérez-Alonso, M.-M.; Sánchez-Parra, B.; Ortiz-García, P.; Santamaría, M.E.; Díaz, I.; Pollmann, S. Jasmonic Acid-Dependent MYC Transcription Factors Bind to a Tandem G-Box Motif in the *YUCCA8* and *YUCCA9* Promoters to Regulate Biotic Stress Responses. *Int. J. Mol. Sci*. **2021**, *22*, 9768.
56. Li, Y.; Yu, Y.; Liu, X.; Zhang, X.; Su, Y. The *Arabidopsis* MATERNAL EFFECT EMBRYO ARREST45 protein modulates maternal auxin biosynthesis and controls seed size by inducing *AINTEGUMENTA. Plant Cell,* **2021**, *33*, 1907-1926.
57. Cheng, Y.; Dai, X.; Zhao, Y. Auxin synthesized by the YUCCA flavin monooxygenases is essential for embryogenesis and leaf formation in *Arabidopsis*. *Plant Cell*, **2007**, *19,* 2430-2439.
58. Yao, X.; Tian, L.; Yang, J.; Zhao, Y.; Zhu, Y.; Dai, X., Zhao, Y., Yang, Z. Auxin production in diploid microsporocytes is necessary and sufficient for early stages of pollen development. *PLoS Genet.* **2018**, *14*, e1007397.
59. Li, L.; Qin, G.; Tsuge, T.; Hou, X.; Ding, M.; Aoyama, T.; Oka, A.; Chen, Z.; Gu, H.; Zhao, Y.; et al. SPOROCYTELESS modulates YUCCA expression to regulate the development of lateral organs in *Arabidopsis. New Phytol.* **2008**, *179,* 751-764.
60. Lee, M.; Jung, J.; Han, D.; Seo, P.; Park, W.; Park, C. Activation of a flavin monooxygenase gene YUCCA7 enhances drought resistance in *Arabidopsis. Comparative Study.* **2012**, *235*, 923-938.
61. Zhao, Y.; Song, S.; Guo, Y.; Tian, Z.; Shang, Y.; Ding, Y.; Li, X.; Zhao, L.; Zhang, H. Overexpression of auxin synthesis gene *PagYUC6a* in poplar (*Populus alba* × *P. glandulosa*) enhances salt tolerance. *Int J Biol Macromol.* **2025**, *311,* 143712.
62. Lorrai, R.; Boccaccini, A.; Ruta, V.; Possenti, M.; Costantino, P.; Vittorioso, P. Abscisic acid inhibits hypocotyl elongation acting on gibberellins, DELLA proteins and auxin. *AoB Plants*. **2018**, *10*, ply061.
63. Voorrips, R.E. MapChart: Software for the graphical presentation of linkage maps and QTLs. *J. Hered*. **2002**, *93*, 77–78
64. Kumar, S.; Stecher, G.; Li, M.; Knyaz, C.; Tamura, K. MEGA X: Molecular evolutionary genetics analysis across computing platforms. *Mol. Biol. Evol.* **2018**, *35*, 1547–1549.
65. Wilkins, M.R.; Gasteiger, E.; Bairoch, A.; Sanchez, J.C.; Williams, K.L.; Appel, R.D.; Hochstrasser, D.F. Protein identification and analysis tools in the ExPASy server. *Methods Mol. Biol.* **1999**, *112*, 531–552.
66. Bailey, T.L.; Boden, M.; Buske, F.A.; Frith, M.; Grant, C.E.; Clementi, L.; Ren, J.; Li, W.W.; Noble, W.S. MEME SUITE: Tools for motif discovery and searching. *Nucleic Acids Res.* **2009**, *37*, W202–W208.
67. Hu, B.; Jin, J.; Guo, A.Y.; Zhang, H.; Luo, J.; Gao, G. GSDS 2.0: An upgraded gene feature visualization server. *Bioinformatics* **2015**, *31*, 1296–1297.

 doi:10.20944/preprints202512.1329.v1

68. Wang, Y.; Tang, H.; DeBarry, J.D.; Tan, X.; Li, J.; Wang, X.; Lee, T.H.; Jin, H.; Marler, B.; Guo, H.; Kissinger, J.C. MCScanX: A toolkit for detection and evolutionary analysis of gene synteny and collinearity. *Nucleic Acids Res*. **2012**, *40*, e49.
69. Chen, C.; Wu, Y.; Li, J.; Wang, X.; Zeng, Z.; Xu, J.; Liu, Y.; Feng, J.; Chen, H.; He, Y.; Xia, R. TBtools-II: A "one for all, all for one" bioinformatics platform for biological big-data mining. *Mol. Plant*. **2023**, *16*, 1733–1742.
70. Wang, D.; Zhang, Y.; Zhang, Z.; Zhu, J.; Yu, J. KaKs_Calculator 2.0: A Toolkit incorporating gamma-series methods and sliding window strategies. *Genom. Proteom. Bioinform*. **2010**, *8*, 77–80.
71. Clevenger, J.; Chu, Y.; Scheffler, B.; Ozias-Akins, P. A developmental transcriptome map for allotetraploid *Arachis hypogaea*. *Front. Plant Sci*. **2016**, *7*, 1446.
72. Li, L.; Cui, S.; Dang, P.; Yang, X.; Wei, X.; Chen, K.; Liu, L.; Chen, C.Y. GWAS and bulked segregant analysis reveal the Loci controlling growth habit-related traits in cultivated Peanut (*Arachis hypogaea* L.). BMC Genom. **2022**, *23*, 403.
73. Li, J.; Ma, Y.; Hu, M.; Zhao, Y.; Liu, B.; Wang, C.; Zhang, M.; Zhang, L.; Yang, X.; Mu, G. Multi-omics and miRNA interaction joint analysis highlight new insights into anthocyanin biosynthesis in peanuts (*Arachis hypogaea* L.). *Front. Plant Sci.* **2022**, *13*, 818345.
74. Livak, K.J.; Schmittgen, T.D. Analysis of relative gene expression data using real-time quantitative PCR and the 2(-Delta Delta C(T)) Method. *Methods* **2001**, *25*, 402–408.